Study of ICRF Heating Characteristics of Various Antenna in the Large Helical Device

S. Kamio[1], T. Seki[1], K. Saito[1], H. Kasahara[1], R. Seki[1], G. Nomura[1], M. Goto[1], M. Osakabe[1], T. Mutoh[1], and LHD Experiment Group[1]

[1] *National Institute for Fusion Science, Toki 509-5292, Japan*

Ion cyclotron range of frequencies (ICRF) heating is studied using three types of antenna in the Large Helical Device (LHD) shown in Fig. 1. As shown in Fig. 1, One toroidal array antenna (HAS antenna (a)) which can change the parallel wave number $k_{//}$ and two poloidal array antennas (FAIT antenna (b) and PA antenna (c)). FAIT antenna has large power density with the compact head, and high loading resistance with attached the field aligned impedance transformer. PA antenna does not have faraday shield (FS) because recently removed to investigate the effect of the removing the FS. With these antennas, minority ion heating is adopted in helium majority and hydrogen minority plasma in the LHD experiment. In the ICRF minority ion heating, the ICRF heating efficiency strongly depends on the minority ion ratio. The heating efficiency also depends upon the resonance layer, plasma loading, plasma parameter, and antenna shape such as with/without faraday shield (FS) because these parameters change the fast ion tail, the absorption layer and/or heating power to peripheral region. In the recent experimental campaign, the FAIT antenna was installed and the FS on PA antenna was removed, and by the upgrade of the heating devices and the control system, high power ICRF (more than 4 MW) can be injected. Therefore the evaluation of ICRF heating characteristics of various antenna is important in the recent experimental condition.

In order to verify these physical properties, we measured the heating efficiency of ICRF minority ion heating in terms of minority ion ratio, electron density and temperature, magnetic field strength, ICRF phase, and plasma-antenna distance in the short pulse (less than 10 sec) and in the long pulse (approximately 40 sec) discharges. In the experiments, we investigated using various diagnostics such as silicon-diode-based fast neutral analyser (Si-FNA)[1] for measuring the fast ion tail, diamagnetic loop, charge exchange spectroscopy with NBI, and Tomson scattering for measuring the plasma stored energy w_p, w_{pi}, and w_{pe}. As a results of these experiments, we summarized the ICRF heating characteristics each three types of antenna. The heating efficiency strongly depends on the plasma density, minority ion ratio, and antenna current phase. They have strong dependence, and results suggest their mutual dependence, however, therefore the conditions are too complex and difficult to make

full database in the limited experimental campaign. Therefore, we summarized the dependences on minority ratio and antenna current phase separately. Figure 2 shows the ICRF heating efficiency dependence on (a) minority ratio and (b) antenna current phase. The heating efficiency were calculated by ICRF power modulation experiments[2]. Here, we used the simple model for calculating the heating efficiency, defined by the ratio of the absorption power P_{abs} and the ICRF P_{ant},

$$\eta \equiv \frac{P_{\mathrm{abs}}}{P_{\mathrm{abs}}} = \frac{\omega}{\sin\delta}\frac{|\delta W_{\mathrm{p}}|}{|\delta P_{\mathrm{abs}}|},$$

We also have to consider the influence of the high-energy ion. The power balance equations are written as

$$\frac{\mathrm{d}W_{\mathrm{tail}}}{\mathrm{d}t} = \eta P_{\mathrm{ant}} - \frac{W_{\mathrm{tail}}}{\tau_{\mathrm{se}}/2} - \frac{W_{\mathrm{tail}}}{\tau_{\mathrm{sHe}}/2} - \frac{W_{\mathrm{tail}}}{\tau_{\mathrm{tail}}},$$

$$\frac{\mathrm{d}W_{\mathrm{bulk}}}{\mathrm{d}t} = \frac{W_{\mathrm{tail}}}{\tau_{\mathrm{se}}/2} + \frac{W_{\mathrm{tail}}}{\tau_{\mathrm{sHe}}/2} - \frac{W_{\mathrm{bulk}}}{\tau_{\mathrm{tail}}}.$$

In this paper, we used simple model for evaluate the heating efficiency, therefore some results may have over estimation.

Toroidal array antenna (HAS) and poloidal array antennas (FAIT and PA) show different dependence upon the minority ratio and antenna current phase. The antenna current phases of good efficiency are shown in Fig. 1 red arrow. Especially, the PA antenna (FS-less) has good efficiency at monopole which cancel the co-axial mode. Because FS-less antenna has large $E_{\perp}$ in front of the antenna head, therefore the cancelling $E_{\perp}$ is important for heating plasma.

High power ICRF injection experiments are demonstrated with various diagnostics, its power and electron density are shown in Fig. 3 (a). Figure 3 (b) and (c) shows the ion and electron temperature, and stored energy. Ion and electron temperature were increased during the increased of the ICRF power, and stored energy of high energy tail calculated by

$$w_{\mathrm{p}} = w_{\mathrm{pi}} + w_{\mathrm{pe}} + w_{\mathrm{pi\_tail}},$$

the stored energy of the high energy ion also increased by increasing the ICRF power. The amount of the high energy particle measured by Si-FNA was increase shown in Fig. 3 (d) however, the effective temperature was almost same. Figure 4 shows the density and temperature profiles. The central ion temperature was increased, and density profile became hollow. We are preparing the ICRF heating calculation, and comparison and evaluation with these experimental results are future works.

[1] M. Osakabe *et al*., Rev. Sci. Instrum. 72, 788-791 (2001)

[2] Y. Torii *et al*., Plasma Phys. Control. Fusion, 43, 1191-1210 (2001)

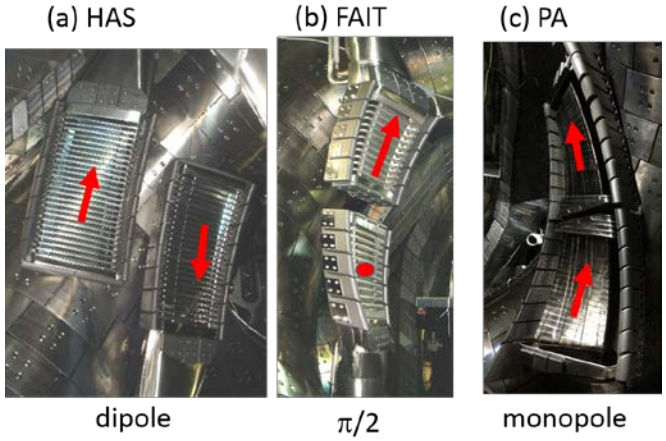

Fig. 1. Pictures of three types of the ICRF antennas, HAS antenna, FAIT antenna, and PA antenna installed in the LHD. Red arrows show the antenna current phase for good heating efficiency.

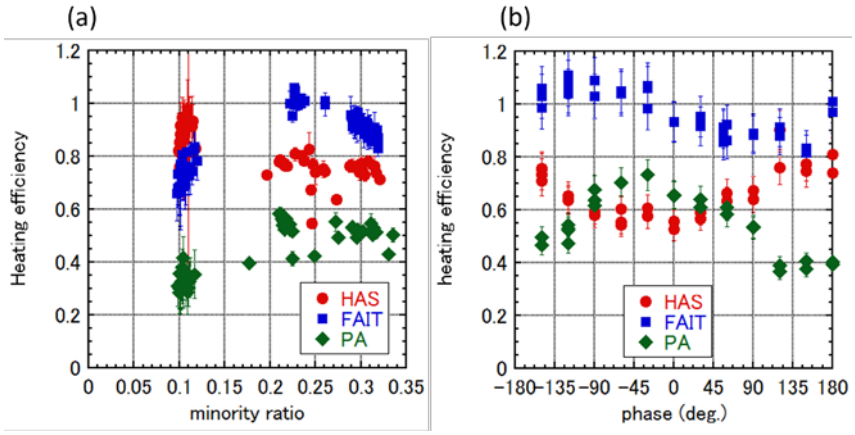

Fig. 2. Heating efficiency of various (a) minority ratio and (b) antenna current phase. As experimental conditions, (a) $n_e = 1 - 1.3 \times 10^{19} \mathrm{m}^{-3}$, and current phases of (HAS, FAIT, PA antenna) are (180, 57, -120 deg.) respectively, and (b) $n_e = 1 - 1.3 \times 10^{19} \mathrm{m}^{-3}$ and minority ratio is 0.2-0.25.

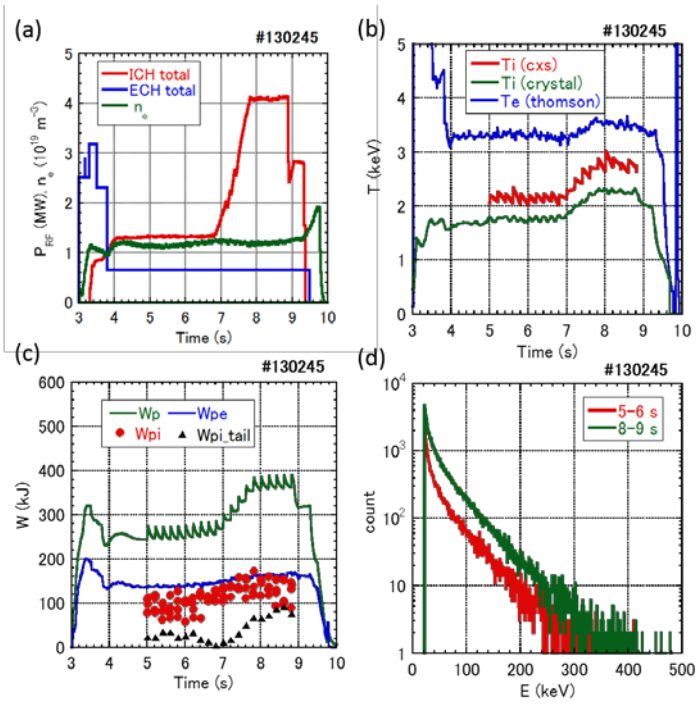

Fig. 3. High power ICRF injection experiments are demonstrated with various diagnostics. (a) The injected RF powers and line averaged electron density, (b) the ion and electron temperature, (c) the stored energy w_p, w_{pe}, and w_{pi} measured by diamagnetic loop, charge exchange spectroscopy, Thomson scattering respectively the w_{pi_tail} is obtained by $w_p - (w_{pi} + w_{pe})$, (d) the results of the high energy particle measurement.

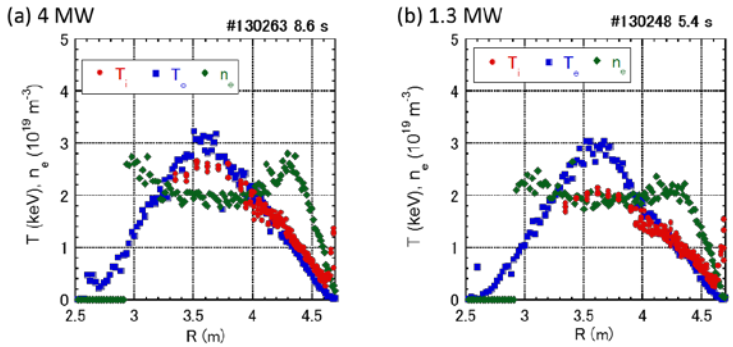

Fig. 4. The results of the electron density profile and the ion and electron temperature profiles measurement in the ICRF (a) high and (b) low power injection.